Cell Proliferation

Cell Prolif., 2010, **43**, 617–628 doi: 10.1111/j.1365-2184.2010.00711.x

Experimental analysis and modelling of *in vitro* HUVECs proliferation in the presence of various types of drugs

L. Mancuso*, M. Scanu*, M. Pisu†, A. Concas† and G. Cao*,†

**Department of Chemical Engineering and Materials, University of Cagliari, Research Unit of Consorzio Interuniversitario Nazionale "La Chimica per l'Ambiente", Piazza d'Armi, Cagliari, Italy, and †CRS4 (Center for Advanced Studies, Research and Development in Sardinia), Piscinamanna Site, Building 1, Pula, Cagliari, Italy*

Received 1 *February* 2010; *revision accepted* 17 *June* 2010

Abstract

Objectives: This study focuses on experimental analysis and corresponding mathematical simulation of *in vitro* HUVECs (human umbilical vein endothelial cells) proliferation in the presence of various types of drugs.

Materials and methods: HUVECs, once seeded in Petri dishes, were expanded to confluence. Temporal profiles of total count obtained by classic haemocytometry and cell size distribution measured using an electronic Coulter counter, are quantitatively simulated by a suitable model based on the population balance approach. Influence of drugs on cell proliferation is also properly simulated by accounting for suitable kinetic equations.

Results and discussion: The models' parameters have been determined by comparison with experimental data related to cell population expansion and cell size distribution in the absence of drugs. Inhibition constant for each type of drug has been estimated by comparing the experimental data with model results concerning temporal profiles of total cell count. The reliability of the model and its predictive capability have been tested by simulating cell size distribution for experiments performed in the presence of drugs. The proposed model will be useful in interpreting effects of selected drugs on expansion of readily available human cells.

Correspondence: G. Cao, Dipartimento di Ingegneria Chimica e Materiali, Università degli Studi di Cagliari, Unità di Ricerca del Consorzio Interuniversitario Nazionale "La Chimica per l'Ambiente", Piazza d'Armi, 09123 Cagliari, Italy. Tel.: +39 070 675 5058; Fax: +39 070 675 5057; E-mail: cao@visnu.dicm.unica.it

Introduction

In the scientific literature, great attention has been devoted to 'pharmacokinetic–pharmacodynamic' modelling and simulation for drug testing and development (1–3). With the progress of computer sciences combined with significant advances in molecular biology and chemistry, new drug development faces the challenge to integrate a huge amount of knowledge accumulated from quantitative structure–activity relationship investigations of any candidate molecule, into large-scale clinical trials in patients (1).

Computer science also appears to be very promising in the field of 'computational toxicology' which may significantly reduce drug development costs (4,5). In the past few years, computational toxicology systems have tremendously increased their predictive capability but the major breakthrough has not been achieved yet because of lack of sufficiently large datasets covering more complex toxicological endpoints (for example, hepatotoxicity, teratogenicity) (5). A comprehensive review of computational methods for toxicity prediction has recently been published (5).

Investigation of inhibitory/toxicity effects of drugs on cell proliferation is undoubtedly useful in drug testing and development. *In vitro* expansion of a cell population is in general an essential step for systematic optimization of culture conditions. At the same time, a targeted investigation on *in vitro* mammalian cell expansion may contribute to evaluation of effects of drugs on both cell metabolism and mitotic processes. A specific study on the effect of drugs during cell proliferation can be particularly useful in oncology and toxicology. Evaluation of intrinsic kinetics of cell proliferation may be performed using a static culture system (that is, in Petri dishes). Interpretation and rationalization of corresponding experiments, which provide a clear contribution to understanding of the complex biological mechanisms involved in stem cell

expansion/differentiation, may be achieved by means of suitable mathematical models (6). In the present study, built upon results of previous studies (6–9), we adopt a population balance equations (PBE) approach to interpret kinetics of an investigated cell system in a quantitative fashion. Usefulness of a PBE approach is strictly linked to the fact that cell population growth and cells' drug uptake may strongly depend upon intrinsic cell properties, distributed among the cell population. As for the PBE approach, age- versus size-based equations, are just one of the latter characteristics considered as distributed over cells, are typically taken into account (10–16).

A comprehensive collection of references in the literature on proliferating cell cultures reported in Mancuso *et al.* (6) demonstrates that the PBE modelling approach has not previously been adopted for quantitatively simulating stem cell culture experiments. Specifically, it has been shown clearly that the proposed population balance modelling approach is much more successful in predicting cell culture expansion with respect to classical generalized logistic equations, which are based on phenomenological representations. *A fortiori*, to the best of our knowledge, no PBE models have previously been developed to quantitatively interpret *in vitro* cell expansion in the presence of drugs. This approach has been followed by means of PBE 'age structure', only to study *in vitro/in vivo* tumour cell growth and expansion in the presence of drugs (17).

The purpose of this study was to formulate, along the lines of previous studies (6), a PBE-based mathematical model to quantitatively describe the response of human cell population growth under the influence of a range of four drugs, captopril, mevinolin, clozapine and risperidone. Clozapine and risperidone are both atypical antipsychotic drugs, and their therapeutic effects are most probably mediated by dopaminergic and serotoninergic activity (18,19). In particular, main pharmacological activities of these drugs include dopamine D2 receptor antagonism and serotonin 5-HT2 blockade. Several studies have demonstrated reduction in cancer risk in patients suffering from schizophrenia when treated with antipsychotic drugs (20–23). Subsequently, several studies have evaluated cytotoxic potential of antipsychotic drugs, using malignant cell lines as well as normal cell lines, such as endothelial lines (24–26). In particular, Asada *et al.* (26) have reported that inhibition of both tumour growth and human umbilical vein endothelial cell (HUVEC) proliferation occurs as result of the blockade of serotoninergic receptor 5-HT2B. Mevinolin is a member of the drug class of statins used for lowering cholesterol in patients with hypercholesterolaemia, to prevent cardiovascular disease. Statins, particularly lipophilic ones, result in cell proliferation inhibition (27,28) due to seemingly multifaceted mechanisms. These include inhibition of cell cycle progression, induction of apoptosis, reduction in cyclooxygenase-2 activity and inhibition of enhancement of angiogenesis (27).

Captopril is an angiotensin-converting enzyme inhibitor (ACE inhibitor) used for treatment of hypertension and some types of congestive heart failure. Mailloux *et al.* (29) have reported that Captopril used at high concentration (10 mM) may be cytotoxic for endothelial cells, while no information, to the best of our knowledge, has been published in the literature concerning effects of Captopril at lower concentrations.

Capability of the proposed model to quantitatively interpret *in vitro* cell expansion in the presence of drugs is evaluated by taking advantage of readily available human cells, here of HUVECs. It is well known that endothelial cells play an important role in physiological haemostasis (30,31) and blood vessel permeability (32–34), and may influence responses of blood vessels to other physiological and pathological stimuli (35,36).

Materials and methods

Human umbilical vein endothelial cells (HUVECs; Clonetics, Lonza, Walkersville, MD, USA) were cultured in endothelial basal medium (EBM; Clonetics, Lonza) supplemented with media-kit EGM-2 (Clonetics, Lonza, Walkersville, MD, USA). At confluence, cells were harvested by treatment with 0.05% trypsin and 0.02% EDTA for 6 min at 37 °C, and replated. Medium was changed every 2 days, and cells from passage 4 were used for proliferation studies.

Count protocol for proliferation studies

HUVECs were plated in 9.2 cm^2 petri dishes (Corning) at 1×10^4 cells/cm^2 density; they were maintained in culture for 6 days. After 1 day's culture, cells were exposed for 24 h to each selected drug. In particular, experiments were performed by adding 40 μM Clozapine, 100 μM Captopril, 1 μM Mevinolin or 40 μM Risperidone, respectively, all obtained from Sigma-Aldrich (St. Louis, MO, USA). Each drug was dissolved in dimethyl sulphoxide, which was used as blank control in all experiments. In particular, experiments were carried out by separately considering a neuropsychiatric drug and a cardiovascular one, while using the same control for both. The first set of experiments was performed by separately adding Clozapine or Captopril into a culture, while in the second, cells were incubated with Risperidone or Mevinolin. At least six independent trials were performed for each investigation.

Cells from three plates for each drug were harvested day-by-day by treatment with 218 μl 0.05% trypsin and 0.02% EDTA for 6 min at 37 °C. The action of trypsin

was stopped with 436 µl of complete medium; Petri dishes were then washed in 436 µl of PBS. Cells were counted electronically on a daily basis using a Coulter counter (Beckman Dickinson, Fullerton, CA, USA) in a total volume of 1.09 ml.

Mathematical modelling and numerical solution

Mathematical simulation, provided by suitable predictive models, represents an important tool to facilitate experiments, helping to find optimal operating conditions and at the same time contributing to understanding of biological mechanisms, which affect cell proliferation kinetics and effects of drug toxicity. The mathematical model proposed in the present study [based on previous studies (6–9)], describes cell proliferation and its size distribution during culture in batch systems. Assuming uniform spatial distribution of spherical cells and neglecting cell death by apoptosis (which is significant only in the case of apoptotic/necrotic cells), the following population balance equation for cell density distribution, $\psi(m, t)$, may be written as (37):

$$\frac{\partial \psi(m,t)}{\partial t} = -\frac{\partial[v\,\psi(m,t)]}{\partial m} + 2\int_m^\infty \psi(m',t)\;\chi_M(m',C_{O_2})\,p(m,m')\;\mathrm{d}m' - \psi(m,t)\,\chi_M(m,C_{O_2}) \quad (1)$$

along with the initial and boundary conditions:

$$\psi(m,\,t) = \psi_0(m), \quad \text{for } t = 0 \text{ and } m > 0, \quad (2)$$

$$\psi(m,\,t) = 0, \quad \text{for } t > 0 \text{ and } m = 0. \quad (3)$$

The left-hand-side of eqn (1) represents temporal variation in cell density distribution $\psi(m, t)$, while terms appearing in the right-hand-side represent cell population growth, cell birth where two daughter cells are obtained by division of a larger mother cell, and disappearance of mother cells due to mitosis, respectively. In eqn (1), χ_M is the cell division function, $p(m, m')$ represents the unequal partitioning distribution of a mother cell of mass m' into daughters of mass m, and C_{O_2} is the oxygen concentration in the culture medium. In eqn (2), $\psi_0(m)$ represents the initial distribution of cells, while the physical meaning of the boundary condition for the PBE model given by eqn (3) is that there exists no cell of zero mass at any time (cf. 12).

The adopted PBE model considers cell mass as internal coordinate as age-structured PBE models can not be validated through comparison with experimental data due to the well-known inability to easily and confidently measure age distribution within a population of cells (cf. 11,12,16). Unequal partitioning distribution of mother cell into daughters, $p(m,m')$, proposed by Hatzis *et al.* (38), is taken into account:

$$p(m,m') = \frac{1}{\beta(q,q)}\frac{1}{m'}\left(\frac{m}{m'}\right)^{q-1}\left(1-\frac{m}{m'}\right)^{q-1}, \quad (4)$$

where $\beta(q,q)$ is the symmetrical beta function:

$$\beta(q,q) = \frac{(\Gamma(q))^2}{\Gamma(2\,q)}, \quad (5)$$

and $\Gamma(q)$ is the gamma function:

$$\Gamma(q) = \int_0^{+\infty} s^{q-1}\,\mathrm{e}^{-s}\,\mathrm{d}s. \quad (6)$$

The cell division function, χ_M, may be expressed by means of the following equation derived from Eakman *et al.* (10):

$$\chi_M(m, C_{O_2}) = v(m, C_{O_2}) \times \gamma_M(m), \quad (7)$$

where

$$\gamma_M(m) = \frac{f(m)}{1 - \int_0^m f(m')\mathrm{d}m'} \quad (8)$$

In particular, if it is assumed that cell division occurs only when a cell reaches a critical mass, the probability density function of a cell of mass m to divide, $f(m)$ may be represented by a normal distribution of dividing mass around the average value μ:

$$f(m) = \frac{1}{\sqrt{2\pi\sigma^2}}\exp\frac{-(m-\mu)^2}{2\sigma^2} \quad (9)$$

being the variance indicated as σ (cf. 10,12). The cell division function, χ_M, which expresses the cell mitotic rate, as shown in eqn (7), increases if the growth rate v is augmented, coherently with the adoption of a mass-based distribution of cells at mitosis ($f(m)$), because by increasing the growth of cell mass, the deterministic or statistical condition at the critical mass for the occurrence of cell division is reached faster.

According to the postulate of von Bertalanffy (39), the time rate of change of cell mass, v, may be written as follows:

$$v(m,C_{O_2}) = \left(\frac{3}{d_c}\right)^{2/3}(4\pi)^{1/3}m^{2/3}\frac{\mu' C_{O_2}}{C_m + C_{O_2}}\Phi - \mu_c m, \quad (10)$$

where the anabolic (positive) term for a single cell is proportional to its surface area ($m^{2/3}$), while the catabolic one (negative) is proportional to cell mass, m (cf. 8,37). In eqn (10), the limiting supply of oxygen (nutrient) is taken into account by a classic Monod kinetics (cf. 10,40). As the experimental procedure adopted in this study guarantees

a supply of constant concentration of nutrients to the expanding culture, the relevant oxygen material balance is not taken into account. As discussed in a previous study (6), to simulate contact inhibition, which progressively slows down culture expansion when reaching the confluence in the Petri dish as proliferation progresses, a limiting factor ($\Phi(t) \leq 1$) appearing in the anabolic term is considered. As a consequence, according to eqn 7, this limiting factor reduces not only the cell mass growth rate but also the cell division function, χ_M, i.e. the rate of cell proliferation. As HUVECs used in this study distribute themselves on a monolayer, it is possible to consider a two-dimensional scheme to account for contact inhibition effect. Along these lines, the limiting factor $\Phi(t)$ of eqn (10) may be related to the available superficial area between cells on the Petri dish surface. Thus, the geometric limiting factor may be defined through the following power law (6):

$$\Phi(t) = \left[1 - \frac{\varphi(t)}{\varphi_a}\right]^{\alpha_P}, \tag{11}$$

where $\varphi(t)$ represents the Petri surface occupied by cells and interstices (increasing with time as proliferation progresses), φ_a the uncovered surface (corresponding to the Petri dish area), and α_p an adjustable parameter. Accordingly, the surface occupied by cells and their interstices is proposed to be calculated as the two-dimensional projection of a monolayer culture of spherical cells as follows:

$$\varphi(t) = V \left(\frac{4}{\pi}\right) \left(\frac{3}{4\, d_c}\right)^{2/3} \pi^{1/3} \int_0^\infty m^{2/3}\, \psi(m,t)\, \mathrm{d}m, \tag{12}$$

where the factor $4/\pi$ is the ratio between the surface of a square (i.e. cell and interstices) and the corresponding inscribed circle (i.e. two-dimensional projection of a spherical cell), while V is the cultivation volume and d_c is the cell mass density. Equation (12) could be easily modified to account for cell adhesion, stretching and deformation (cf. 41). However, this aspect is beyond the aim of the present study. Equation (12) allows one to specify that the surface extension of the Petri dish used for cultivation is characterized by a maximum available surface for monolayer growing cells (and interstices between them), which is proportional to the moment of order 2⁄3 of the mass-based distribution.

It should be noted that without distinguishing among cells belonging to different cell cycle phases and by neglecting complex intra- and extracellular biochemistry, the proposed model permits one to basically track the essential features of the proliferation process taking place and to simulate the confluence limitation arising from contact inhibition when a saturation level is reached within the Petri dish (cf. 6).

When a specific drug characterized by concentration C_I is added to the culture medium, eqn (10) may be rewritten by accounting for the drug inhibitory effect, through the introduction of the term $\left(1 + C_I/K_I\right)^{-1}$, according to (42):

$$v(m, C_{O_2}) = \left(\frac{3}{d_c}\right)^{2/3} (4\,\pi)^{1/3} m^{2/3} \left(\frac{1}{1 + \frac{C_I}{K_I}}\right) \frac{\mu'\ C_{O_2}}{C_m + C_{O_2}}\ \Phi - \mu_c m, \tag{13}$$

where K_I is the inhibition constant.

It should be noted that trypsinization and consequent Coulter counting are not accounted for in the model. While such a task is most probably not trivial and might be the subject of future studies, the adopted experimental procedure is quite classical and generally accepted in the literature. Consequently, such experimental manipulations are not taken into account in the model formulation. Equation (1) is a partial integro-differential equation in the variables t and m along with the initial and boundary conditions eqns (2) and (3) respectively. In particular, the mass domain of integration ranges hypothetically from zero to $+\infty$. This upper limit is obviously not tractable by numerical analysis. A relatively high value may be safely chosen if cell distribution $\psi(m,t)$ is entirely contained in the corresponding m domain during its dynamic behaviour. In this study, the upper limit was set equal to 16 ng, which corresponds to a cell of diameter approximately 25 μm. The numerical solution of partial integro-differential eqn (1) along with the initial and boundary conditions represented by eqns (2) and (3) is performed by means of the method of lines (43). After the choice of the upper limit, the mass domain is divided using a constant step size mesh, and only the partial derivative with respect to m is discretized by backward finite difference. Then, the partial integro-differential eqn (1) is transformed into a system of ordinary differential equations in time, which is integrated by means of standard numerical libraries (Gear method, IMSL) as an initial value problem. A total of 101 grid points (including the first one which corresponds to $m = 0$) in the mass domain are typically used for numerically solving the PBE model, because finer grids did not provide significant improvements in accuracy. In particular, we considered, as discretized mass domain, the following uniform grid: $m_j = (j-1)\left(16/100\right)$ for $j = 1, \ldots, N_m = 101$. Details of the used numerical method and the discretizing scheme are reported elsewhere (6).

The fitting procedure adopted for determining the unknown, adjustable parameters μ', σ and α_P, when drugs are not added to the cell culture (CTRL run), consisted of minimizing a specific objective function. At the

i-th time instant, the total number of cells, $N_{\mathrm{calc},i}$, and the cell distribution, $P_{\mathrm{calc},i,k}$, in terms of cell percentage as a function of k-th cell mass m_k to be compared with experimental data, are calculated as follows:

$$N_{\mathrm{calc},i} = V \int_0^{\infty} \psi(m,t)\mathrm{d}m, \tag{14}$$

$$P_{\mathrm{calc},i,k} = 100\frac{V\psi(m_k,t)}{N_{\mathrm{calc},i}}(m_k - m_{k-1}),$$
$$k = 2,\ldots N_d = 301, \tag{15}$$

where m_k is the mass corresponding to the generic cell diameter d_k on the basis of the experimental histogram bins (i.e. $m_k = 4/3\pi\left(d_k/2\right)^3 d_c$ for the case of spherical cells with mass density d_c) and $\psi(m_k,t)$ the density distribution as a function of k-th cell diameter d_k. It should be noted that when $k = 1$, $d_k = 0$ ($m_k = 0$), $\psi(m_k,t) = 0$ and $P_{\mathrm{calc},i,k} = 0$, coherently with the boundary condition (3). The function $\psi(m_k,t)$, for $k = 2, \ldots, N_d = 301$, has been calculated by means of suitable interpolation procedure (subroutine DQDVAL, IMSL) from the density distribution provided by the model, $\psi(m_j,t)$, where $m_j = (j-1)\left(16/100\right)$ for $j = 2, \ldots, N_m = 101$. Also in this case, when $j = 1$, $m_j = 0$ and $\psi(m_j,t) = 0$ accordingly to the boundary condition (3).

The objective function F may be then written as follows:

$$F = \sum_{i=1}^{N_t} \frac{\left(N_{\mathrm{exp},i} - N_{\mathrm{calc},i}\right)^2}{N_{\mathrm{exp},i}^2} + \sum_{i=1}^{N_t}\left(\frac{\sum_k^{N_d}\left(P_{\mathrm{exp},i,k} - P_{\mathrm{calc},i,k}\right)^2}{\sum_j^{N_m} P_{\mathrm{exp},i,k}^2}\right), \tag{16}$$

where index i is related to the cultivation time, index k to the generic cell diameter d_k of the distribution, $N_{\mathrm{exp},i}$ is the experimental cell count, $N_{\mathrm{calc},i}$ the calculated one, and finally, $P_{\mathrm{exp},i,k}$ and $P_{\mathrm{calc},i,k}$ the experimental and calculated cell percentages respectively.

In the case of experiment performed in the presence of drugs, the inhibition constant K_{I} has been estimated by comparing model results and experimental data in terms of total cell count as a function of time. We assume that the main effect of the parameter K_{I} applies on the total cell count and therefore the objective function F in this case is written as follows:

$$F = \sum_{i=1}^{N_t} \frac{\left(N_{\mathrm{exp},i} - N_{\mathrm{calc},i}\right)^2}{N_{\mathrm{exp},i}^2}. \tag{17}$$

The minimization of the objective function F [eqns (16) or (17)] is carried out by means of the Fortran subroutine BURENL, which is based on the least-squares method (cf. 44).

Results and discussion

Experimental data for each experimental run were measured using the electronic Coulter counter, in terms of cell distribution as a function of cell diameter (μm) and in terms of total cell count as a function of culture time.

Initial cell distribution in the absence of drugs (CTRL run) for the experiment performed to test the effect of Clozapine and Captopril, which are added after 1 day of culture, is reported in Fig. 1a. Analogously, the initial cell distribution is reported in Fig. 1b for the experiment performed to test the effect of mevinolin and risperidone. It is worth noting that in our mathematical simulations, the initial time is day one of cultivation as the model does not account for the 'acclimation time' of the cells. In addition, drugs are added only after 1 day of cultivation. From

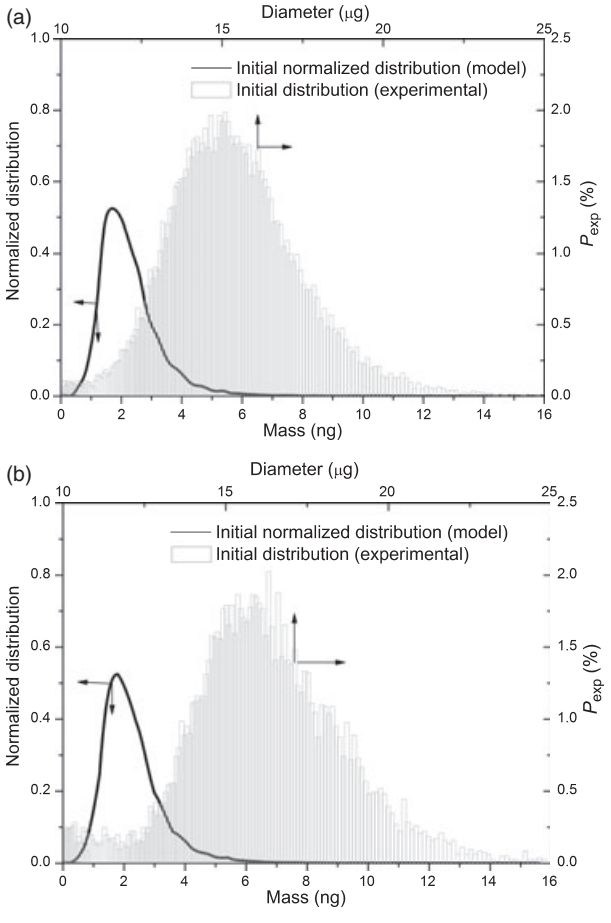

Figure 1. Initial experimental cell size distribution in terms of cell number percentage (histogram) as a function of cell diameter measured using an electronic Coulter counter and model normalized initial distribution for trials performed with no drugs or by adding clozapine or captopril (a) and experiment performed with no drugs or by adding mevinolin or risperidone (b).

Parameter	Value	Unit	Reference
N_0	8.0×10^4 or 9.0×10^4	Cells	This study
ψ_a	920	mm^2	This study
V	1500	mm^3	This study
C_{O_2}	0.203×10^{-6}	$mmol/mm^3$	(45)
C_m	0.006×10^{-6}	$mmol/mm^3$	(46)
d_c	1.14×10^6	ng/mm^3	(47)
μ	4.0	ng	This study
q	40	–	(12)
μ_C	1.0×10^{-3}	1/h	(48)
μ'	1.35×10^2	$ng/(mm^2\ h)$	This study (tuned parameter)
σ	1.57	ng	This study (tuned parameter)
α_P	8.44	–	This study (tuned parameter)
C_I	40×10^{-6}	$\mu mol/mm^3$	This study (clozapine concentration)
K_I	52.5×10^{-6}	$\mu mol/mm^3$	This study (tuned parameter for clozapine)
C_I	100×10^{-6}	$\mu mol/mm^3$	This study (captopril concentration)
K_I	621×10^{-6}	$\mu mol/mm^3$	This study (tuned parameter for captopril)
C_I	1×10^{-6}	$\mu mol/mm^3$	This study (mevinolin concentration)
K_I	1.5×10^{-6}	$\mu mol/mm^3$	This study (tuned parameter for mevinolin)
C_I	40×10^{-6}	$\mu mol/mm^3$	This study (risperidone concentration)
K_I	35.4×10^{-6}	$\mu mol/mm^3$	This study (tuned parameter for risperidone)

Table 1. Model parameters for PBE modelling approach used in the simulation. Parameters μ', σ and α_P, are obtained by fitting model results against experimental data in the absence of the drug. Parameter K_I is obtained by fitting model results against experimental data in terms of cell total count as a function of time when drug is added

Fig. 1, it is possible to notice that the distribution mode is placed at about 15.2 μm. To numerically solve the adopted model, the measured initial cell distribution has to be converted into the number distribution density $\psi_0(m)$, considered as initial condition (cf. eqn (2)). Starting from the histogram reported in Fig. 1a (for the experiments performed to test the effect of clozapine and captopril) and Fig. 1b (for the experiments performed to test the effect of mevinolin and risperidone), the discretized version of the initial cell mass number density distribution is readily obtained as $\psi_0(m_k) = N_{\exp,0}/100\, VP_{\exp,0,k}/(m_k - m_{k-1})$, for $k = 2, \ldots, N_d$ and $m_k = 4/3\pi\left(d_k/2\right)^3 d_c$, for cells of spherical shape, d_k being the generic cell diameter and d_c its mass density. Then, by interpolating through standard mathematical quadratic methods (subroutine DQDVAL, IMSL), the continuous form of ψ_0 may be easily evaluated, so that the corresponding value of $\psi_0(m_j)$ at any j-th mass grid point ($j = 2, \ldots, N_m$) of the uniform mesh numerically adopted for solving the model by the method of lines may be calculated. The normalized initial distribution used during the simulations is depicted in Fig. 1a,b for experiments performed to test the effect of clozapine–captopril and mevinolin–risperidone respectively.

To determine the unknown model parameters by minimizing the objective function defined in eqn (16), model results were fitted against the measured total cell count and cell distribution expressed as number percentage of cell (histogram) as a function of cell diameter. The values of the model parameters used in simulation runs, with $N_0 = 8 \times 10^4$ as initial cell number, are reported in Table 1. It is seen that, some of them are taken from the literature, others are obtained through fitting, while the remaining ones represent operative conditions used experimentally in this study. In particular, the mean of the normal distribution of mitotic fraction [i.e. μ in eqn (9)] is assumed to be equal to about twice the value of the mode of the measured initial distribution shown in Fig. 1a (i.e. μ = 4 ng). This seems a reasonable choice (cf. 6,12). Indeed, as no synchronization by either physical or biochemical means has been performed on the cell population, the mode of the initial distribution should correspond to the mean size of the daughter cells (6). Three parameters, i.e. the proportionality constant 'μ', of cell mass rate, the order α_P of the power law given in eqn (11), and σ, the value of the variance of the normal distribution of dividing mass appearing in eqn (9), have been determined using a nonlinear fitting procedure, where the objective function F is given by eqn (16). Comparison between model results and experimental data (in absence of drugs, CTRL) in terms of total cell number as a function of cultivation time is depicted in Fig. 2, while in Fig. 3, the comparisons in terms of cell percentage distributions (histograms) as a function of cell diameter are reported at various cultivation times. The values of the model parameters obtained through the fitting procedure are reported in Table 1. The good agreement between model results and experimental data demonstrate the validity of the proposed modelling approach. It is important to remark that a specific procedure has been performed to test the stability of the adopted optimization scheme when estimating the model parameter μ', α_P and σ.

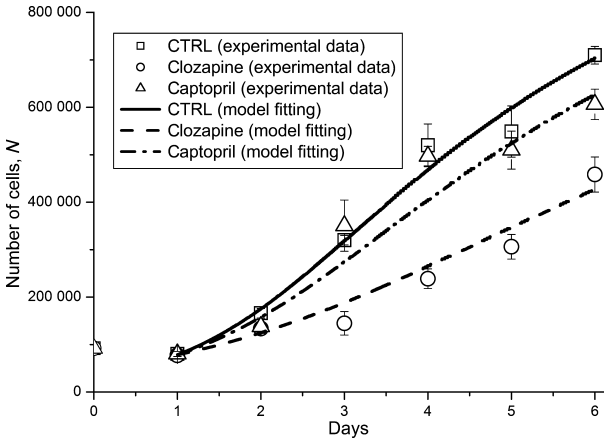

Figure 2. Comparison between model results and experimental data in terms of total cell count cultivated in Petri dishes (CTRL, trial with no drugs).

Specifically, a perturbation noise on the estimated parameter values (from −20% to +20%) has been applied. The solution of the consequent *direct problem* allows one to obtain 'artificial' data, which were used to fit once more the desired parameters (one computation run may take from 12 to 18 h of CPU time in a 32 bit, 3 GHz, dual core PC). No appreciable difference in the obtained parameter values has been observed with respect to those ones used to obtain the 'artificial' data.

From Fig. 2, it may also be observed that the model well interprets the exponential growth, which occurs during the first days of cultivation (up to 2–3 days) and properly simulates the effect of contact inhibition, which arises after about 3 days of cell expansion. The confluence is not fully reached after 6 days of culture and therefore the expansion curve does not display the typical plateau. As it is shown in Fig. 3, the agreement between model results and experimental data is also good in terms of cell

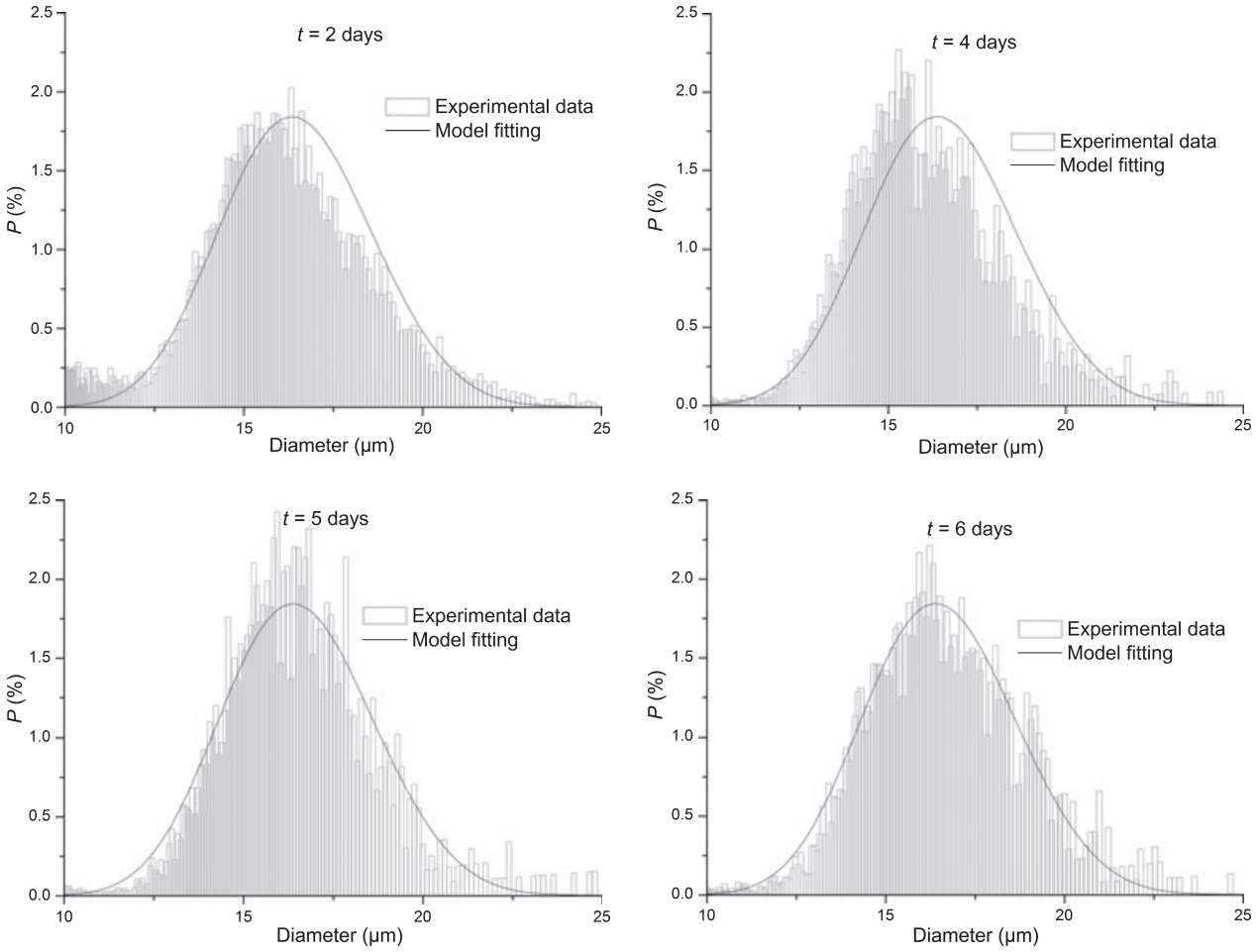

Figure 3. Comparison between model results and experimental data in terms of cell number percentage (histogram) as a function of cell diameter measured using the electronic Coulter counter for the trial where no drugs were added.

percentage distributions (histograms) as a function of cell diameter except for the cell distribution at $t = 4$ days of culture, where the measured cell sizes are shifted towards lower values than those calculated by the adopted model. In Fig. 2, the comparison between model results and experimental data in terms of total cell count as a function of time when selected drugs are added (i.e. clozapine 40 μM and captopril 100 μM, respectively) is also reported.

In this case, for each drug, the parameter K_I has been estimated by a fitting procedure where the objective function F is given by eqn (17) and the corresponding values are reported in Table 1. From Fig. 2, it is possible to observe that there is a good agreement between model results and experimental data (9.7% of relative error for the cell expansion performed in the presence of clozapine and 13% of relative error when captopril is used). Both drugs inhibit cell expansion and this is particularly true for clozapine, which reduces the total cell count of about 40% after 6 days. It should be noticed that in our model, the inhibition of cell growth and proliferation due to the drug presence increases when the ratio C_I/K_I increases (see eqn 13). Correspondingly, in the case of the experiment performed with clozapine, this ratio is equal to 0.76 compared to the value of 0.16 for the experiment performed with captopril.

The model's predictive capability is displayed in Figs 4 and 5 in terms of cell distribution (percentage as a function of cell diameter) for experimental runs performed with clozapine and captopril respectively. The agreement between model results and experimental data is acceptable for the cultivation time considered.

The same approach has been followed to investigate the effect of Mevinolin and Risperidone on cell proliferation and growth, the initial cell number being equal to 9×10^4 (Table 1). In this case, the experimental data in

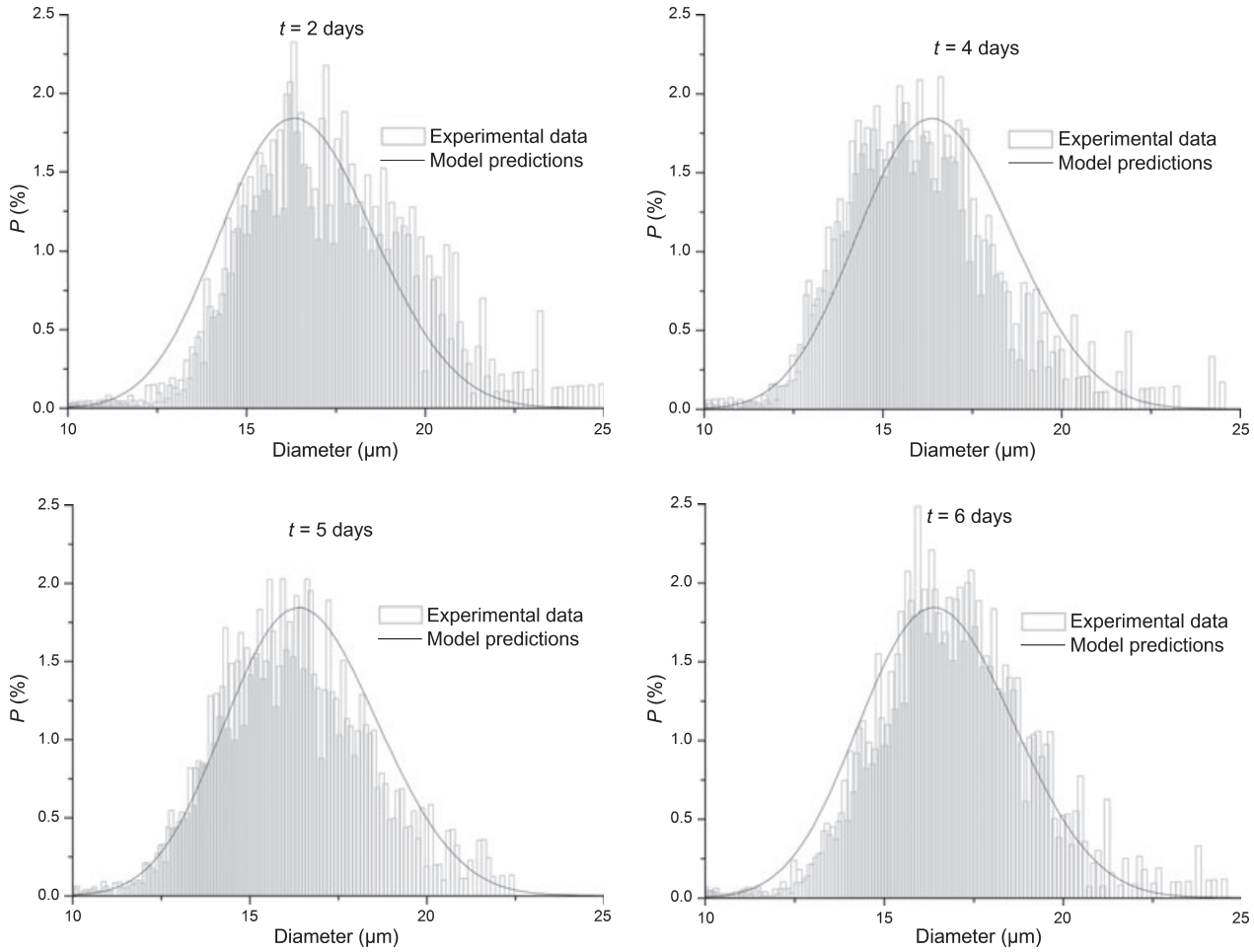

Figure 4. Comparison between model predictions and experimental data in terms of cell number percentage (histogram) as a function of cell diameter measured using the electronic Coulter counter for the trial performed by adding clozapine.

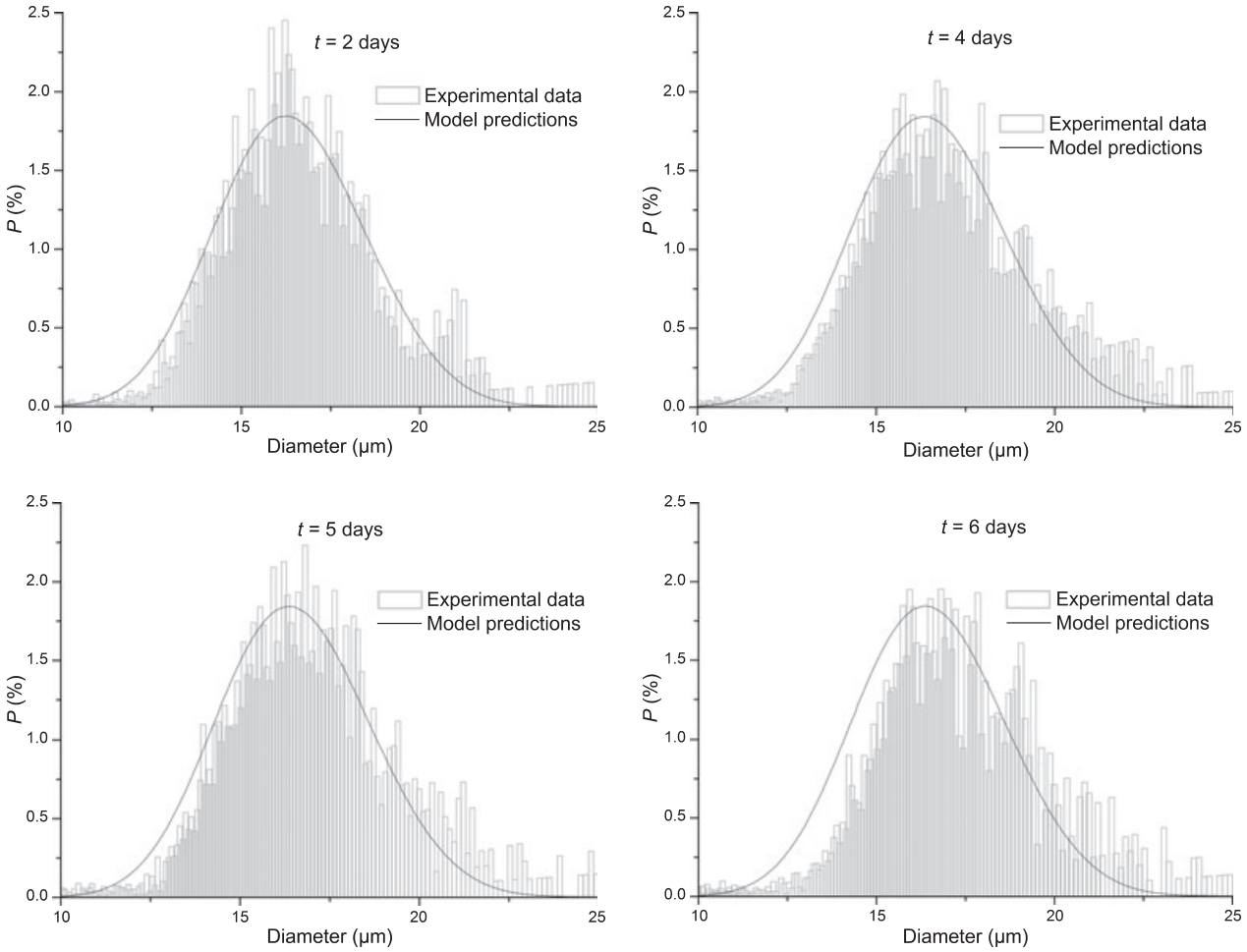

Figure 5. Comparison between model predictions and experimental data in terms of cell number percentage (histogram) as a function of cell diameter measured using the electronic Coulter counter for the trial performed by adding captopril.

the absence of drugs (CTRL) are entirely predicted through our model by considering the corresponding parameters reported in Table 1, which have been accordingly maintained fixed except for the initial cell number. The corresponding comparison between model predictions and experimental data (in the absence of drugs, CTRL) in terms of total cell number as a function of cultivation time is depicted in Fig. 6, while the comparison in terms of cell percentage distributions (histograms) as a function of cell diameter is reported in Fig. 7a, for the case of 2 days of cultivation time. For brevity, the comparisons between experimental data and model results for other cultivation times, which display similar behaviour to that one shown in Fig. 7a, are not reported. The good agreement between model results and experimental data confirms the validity of the proposed model. As for the experimental run described previously, the confluence is not reached after 6 days of cell expansion but the effect of cell contact inhibition appears evident from 2 to 3 days of cultivation. Figure 6 also shows the comparison between model results and experimental data in terms of total cell count as a function of time when 1 μM mevinolin or 40 μM risperidone is added after 1 day of cultivation.

For each drug, the parameter K_I has been estimated by a fitting procedure where the objective function F given by eqn (17) is taken into account. The corresponding values are reported in Table 1. As shown in Fig. 6, a good agreement between model results and experimental data (10.6% of relative error for the cell expansion performed in the presence of mevinolin and 8.7% when risperidone is used) is obtained. Both drugs inhibit cell expansion, being the major effect due to risperidone. In fact $C_I/K_I = 1.13$ for the case of risperidone while it is equal to 0.67 in the case of the experiment performed by adding mevinolin. The predictive capability of the model

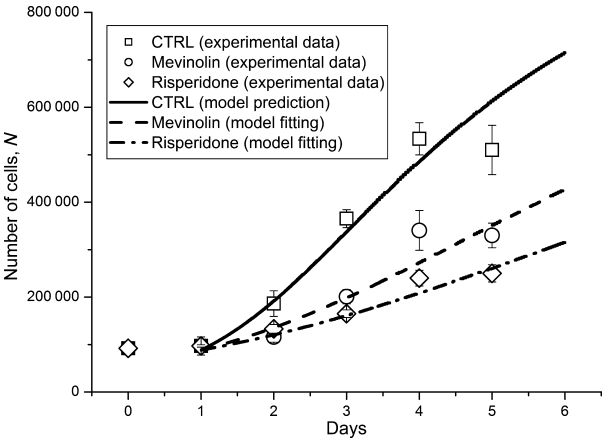

Figure 6. Comparison between model results and experimental data in terms of total cell count when cultivated in Petri dishes (CTRL, trial with no drugs).

is demonstrated in Fig. 7b,c where the comparison between model results and experimental data is shown in terms of cell distribution (percentage) as a function of cell diameter when mevinolin (Fig. 7b) or risperidone (Fig. 7c) is added during cell cultivation. For brevity, the comparison between experimental data and model prediction is shown only after 2 days of cultivation. Similar results have been obtained for other cultivation times investigated. The agreement between model results and experimental data, as illustrated in Fig. 7b,c, seems acceptable.

It is worth noting that the effect of selected drugs on HUVEC proliferation quantitatively described in this study (cf. Figs 2 and 6) has a sound biological justification.

Antipsychotic drugs, as discussed above, have significant effect on cell proliferation by means of dopamine D2

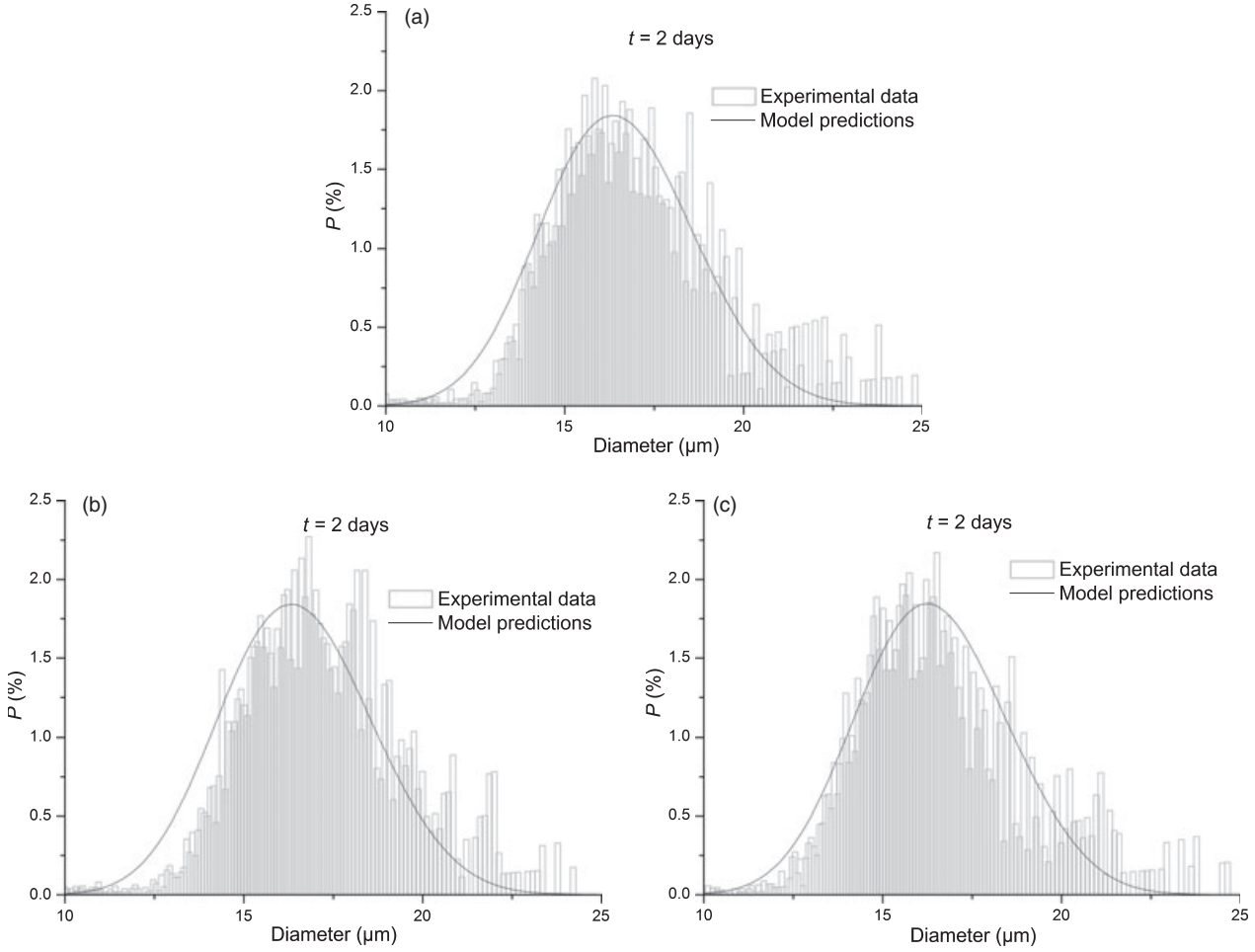

Figure 7. Comparison between model results and experimental data in terms of cell number percentage (histogram) as a function of cell diameter after 2 days of cultivation measured using the electronic Coulter counter; (a) CTRL, trial with no drugs; (b) trial performed by adding mevinolin; (c) trial performed by adding risperidone.

receptor antagonism and serotonin 5-HT2 blockade. This fact may explain the inhibition effect of antipsychotic drugs such as clozapine (Fig. 2) and risperidone (Fig. 6) on HUVEC proliferation.

For what concern the experiments performed by adding Mevinolin in the culture medium, our results demonstrate that this drug inhibits endothelial cells proliferation (Fig. 6), according to the well known evidence that statins give rise to cell proliferation inhibitions, as discussed in the introduction.

Regarding the effect of Captopril on HUVEC culture, no consideration can be made because, to the best of our knowledge, no information concerning this drug is available when used at low concentration as in our experiments.

Concluding remarks

Experimental analysis, mathematical modelling and simulation of *in vitro* HUVEC proliferation in the presence of various types of drugs used in neuropsychiatry and cardiology were addressed in this study. The temporal profiles of total cell count and the cell size distribution are quantitatively interpreted by a population balance model capable of taking into account cell contact inhibition at confluence as well as the effect of some types of drugs on cell proliferation. The proposed model based on a PBE approach represents to our knowledge a first step towards quantitative interpretation of HUVEC proliferation in the presence of various types of drugs, which can be extended to other readily available human cells.

Acknowledgements

Ministero dell'Università e della Ricerca (MUR), Italy, is gratefully acknowledged for the financial support of the project SVIFASTA. Regarding the latter, one of us (G.C.) would like to thank the scientific coordinator, Dr Luca Pani, for his dedicated activity.

This study has been also carried out with the financial contribution of the Sardinian Regional Authorities.

References

1 Balant LP, Gex-Fabry M (2000) Modelling during drug development. *Eur. J. Pharm. Biopharm.* **50**, 13–26.
2 Aarons L, Karlsson MO, Mentre F, Rombout F, Steimer JL, van Peer A (2001) Role of modelling and simulation in phase I drug development. *Eur. J. Pharm. Sci.* **13**, 115–122.
3 Bonate P (2006) *Pharmacokinetic Pharmacodynamic Modeling and Simulation*. New York: Springer-Verlag.
4 Hall AH (1998) Computer modeling and computational toxicology in new chemical and pharmaceutical product development. *Toxicol. Lett.* **102–103**, 623–626.
5 Muster W, Breidenbach A, Fischer H, Kirchner S, Muller L, Pahler A (2008) Computational toxicology in drug development. *Drug Discov. Today* **13**, 303–310.
6 Mancuso L, Liuzzo MI, Fadda S, Pisu M, Cincotti A, Arras M *et al.* (2009) Experimental analysis and modeling of *in vitro* mesenchymal stem cells proliferation. *Cell Prolif.* **42**, 602–616.
7 Pisu M, Lai N, Cincotti A, Delogu F, Cao G (2003) A simulation model for the growth of engineered cartilage on polymeric scaffolds. *Int. J. Chem. React. Eng.* **1**, 1–13.
8 Pisu M, Lai N, Cincotti A, Concas A, Cao G (2004) Model of engineered cartilage growth in rotating bioreactors. *Chem. Eng. Sci.* **59**, 5035–5040.
9 Pisu M, Concas A, Lai N, Cao G (2006) A novel simulation model for engineered cartilage growth in static systems. *Tissue Eng.* **12**, 2311–2320.
10 Eakman JM, Fredrickson AG, Tsuchiya HM (1966) Statistics and dynamics of microbial cell populations. *Bioeng. Food Process.* **62**, 37–49.
11 Liou JJ, Srienc F, Fredrickson AG (1997) Solutions of population balance models based on a successive generations approach. *Chem. Eng. Sci.* **52**, 1529–1540.
12 Mantzaris NV, Liou JJ, Daoutidis P, Srienc F (1999) Numerical solution of a mass structured cell population balance in an environment of changing substrate concentration. *J. Biotechnol.* **71**, 157–174.
13 Abu-Absi N, Srienc F (2002) Instantaneous evaluation of mammalian cell culture growth rates through the analysis of the mitotic index. *J. Biotechnol.* **95**, 63–84.
14 Cipollina C, Vai M, Porro D, Hatzis C (2007) Towards understanding of the complex structure of growing yeast populations. *J. Biotechnol.* **128**, 393–402.
15 Mantzaris NV (2006) Stochastic and deterministic simulations of heterogeneous cell population dynamics. *J. Theor. Biol.* **241**, 690–706.
16 Sherer E, Tocce E, Hannemann RE, Rundell AE, Ramkrishna D (2008) Identification of age-structured models: cell cycle phase transitions. *Biotechnol. Bioeng.* **99**, 960–974.
17 Hinow P, Wang SE, Arteaga CL, Webb GF (2007) A mathematical model separates quantitatively the cytostatic and cytotoxic effects of a HER2 tyrosine kinase inhibitor. *Theor. Biol. Med. Model.* **4**, 14. http://www.tbiomed.com.
18 Meltzer HY (1989) Clinical studies on the mechanism of action of Clozapine: the dopamine-serotonine hypothesis of schizophrenia. *Psychopharmacology* **99**(Suppl.), S18–S27.
19 Janssen PA, Niemegeers CJ, Awouters F, Schellekens KH, Megens AA, Meert TF (1988) Pharmacology of Risperidone (R 64 766), a new antipsychotic with serotonin-S2 and dopamine-D2 antagonistic properties. *J. Pharmacol. Exp. Ther.* **244**, 685–693.
20 Mortensen PB (1989) The incidence of cancer in schizophrenic patients. *J. Epidemiol. Community Health* **43**, 43–47.
21 Jeste DV, Gladsjo JA, Lindamer LA, Lacro JP (1996) Medical comorbidity in schizophrenia. *Schizophr. Bull.* **22**, 413–430.
22 Catts VS, Catts SV (2000) Apoptosis and schizophrenia: is the tumour suppressor gene, p53, a candidate susceptibility gene? *Schizophr. Res.* **81**, 47–63.
23 Carney CP, Jones L, Woolson RF (2006) Medical comorbidity in women and men with schizophrenia: a population-based controlled study. *J. Gen. Intern. Med.* **21**, 1133–1137.
24 Pakala R, Benedict CR (1998) Effect of serotonin and thromboxane A2 on endothelial cell proliferation: effect of specific receptor antagonists. *J. Lab. Clin. Med.* **131**, 527–537.
25 Wiklund ED, Catts VS, Catts SV, Ng TF, Whitaker NJ, Brown AJ *et al.* (2010) Cytotoxic effects of antipsychotic drugs implicate

cholesterol homeostasis as a novel chemotherapeutic target. *Int. J. Cancer* **126**, 28–40.
26 Asada M, Ebihara S, Yamanda S, Niu K, Okazaki T, Sora I *et al.* (2009) Depletion of serotonin and selective inhibition of 2B receptor suppressed tumor angiogenesis by inhibiting endothelial nitric oxide synthase and extracellular signal-regulated kinase 1/2 phosphorylation. *Neoplasia* **11**, 408–417.
27 Davignon J, Mabile L (2001) Mechanisms of action of statins and their pleiotropic effects. *Ann. Endocrinol.* **62**, 101–112.
28 Depasquale I, Wheatley DN (2006) Action of Lovastatin (Mevinolin) on an in vitro model of angiogenesis and its co-culture with malignant melanoma cell lines. *Cancer Cell Int.* **6**, 9. http://www.cancerci.com/content/6/1/9.
29 Mailloux A, Deslandes B, Vaubourdolle M, Baudin B (2003) Captopril and enalaprilat decrease antioxidant defences in human endothelial cells and are unable to protect against apoptosis. *Cell Biol. Int.* **27**, 825–830.
30 Todd AS (1959) The histological localisation of fibrinolysin activator. *J. Pathol. Bacteriol.* **78**, 281–283.
31 Spaet TH, Erickson RB (1966) The vascular wall in the pathogenesis of thrombosis. *Thromb. Diath. Haemorrh.* **21**(Suppl.), 67–86.
32 Gimbrone MA, Aster RH, Cotran RS, Corkery J, Jandl JH, Folkman J (1969) Preservation of vascular integrity in organs perfused in vitro with a platelet-rich medium. *Nature* **222**, 33–36.
33 Gore I, Takada M, Austin J (1970) Ultrastructural basis of experimental thrombocytopenic purpura. *Arch. Pathol.* **90**, 197–201.
34 Roy AJ, Djerassi I (1972) Effects of platelet transfusions: plug formation and maintenance of vascular integrity. *Proc. Soc. Exp. Biol. Med.* **139**, 137–142.
35 Mustard JF, Packham A (1971) Role of platelets and thrombosis in atherosclerosis. In: Brinkhaus KM, Shermer RW, Mostofi FK, eds. *The Platelet*, pp. 215–232. Baltimore: The Williams & Wilkins Co.
36 Didisheim P (1972) Animal models useful in the study of thrombosis and antithromhotic agents. In: Spaet TH, ed. *Progress Hemostasis and Thrombosis*, pp. 165–197. New York: Grune & Stratton, Inc.
37 Himmelblau DM, Bischoff KB (1968) *Process Analysis and Simulation: Deterministic Systems*. New York: Wiley J.
38 Hatzis C, Srienc F, Fredrickson AG (1995) Multistaged corpuscolar models of microbial growth: Monte Carlo simulations. *Biosystems* **36**, 19–35.
39 von Bertalanffy L (1957) Quantitative laws in metabolism and growth. *Q. Rev. Biol.* **32**, 217–231.
40 Liu YH, Bi JX, Zeng AP, Yuan JQ (2007) A population balance model describing the cell cycle dynamics of myeloma cell cultivation. *Biotechnol. Prog.*, **23**, 1198–1209.
41 Hata N, Hirai H, Kino-oka M, Taya M (2004) Comprehension of and attachment and multiplication properties by observing individual cell behaviors in anchorage-dependent culture. *Biochem. Eng. J.* **20**, 197–202.
42 Schügerl K (1987) *Bioreaction Engineering – Reaction Involving Microorganisms and Cells 1*. New York: Wiley J.
43 Schiesser WE (1991) *The Numerical Method of Lines*. San Diego: Academic Press.
44 Donati G, Buzzi-Ferraris G (1974) A powerful method for Hougen-Watson model parameter estimation with integral conversion data. *Chem. Eng. Sci.* **29**, 1504–1509.
45 Schumpe A, Quicker G, Deckwer DW (1982) Gas solubilities in microbial culture media. *Adv. Biochem. Eng.* **24**, 1–38.
46 Obradovic B, Meldon JH, Freed LE, Vunjak-Novakovic G (2000) Glycosaminoglycan deposition in engineered cartilage: experiments and mathematical model. *AIChE J.* **46**, 1860–1871.
47 Jakob M, Demarteau O, Schafer D, Stumm M, Heberer M, Martin I (2003) Enzymatic digestion of adult human articular cartilage yields a small fraction of the total available cells. *Connect. Tissue Res.* **44**, 173–180.
48 Munteanu SE, Ilic MZ, Handley CJ (2002) Highly sulfated glycosaminoglycans inhibit aggrecanase degradation of aggrecan by bovine articular cartilage explant culture. *Matrix Biol.* **21**, 429–440.

Nomenclature

C_I drug concentration in the culture medium, μmol/mm^3
C_{O_2} concentration of O_2 at saturation condition, mmol/mm^3
C_m oxygen concentration at half-maximal consumption, mmol/mm^3
d cell diameter, μm
d_c mass density, ng/mm^3
F objective function
$f(m)$ division probability density function, 1/ng
K_I inhibition constant, μmol/mm^3
m single cell mass, ng
m' mother cell mass, ng
N cell number, cells
N_d number of cell diameter bins in histogram
N_t number of time instants used during the fitting procedure
N_m number of cell mass grid points
P cell percentage, %
p partitioning function, 1/ng
q coefficient appearing in the symmetric beta function
t time, d
V total cultivation volume, mm^3

Greek letters

α_P order of the power law given in eqn (11)
$\beta(q,q)$ symmetric beta function
ψ occupied area by cells and interstices, mm^2
ψ_a Petri dish area, mm^2
Φ geometric limiting factor
$\Gamma(q)$ gamma function
γ_M distribution defined in eqn (8), 1/ng
μ average mass of dividing cells in eqn (8), ng
μ' maximum rate of cell growth, ng/(mm^2 h)
μ_c catabolic rate, 1/h
v time rate of change of cell mass m, ng/h
σ standard deviation of the Gaussian distribution f(m) defined in eqn (9), ng
χ_M division rate function, 1/h
ψ cell distribution function, cells/(ng mm^3)

Subscripts

Calc calculated value by model
Exp experimental value
i index for generic time instant
j index for generic cell mass
k index for generic cell diameter
0 index for initial time